



ELSEVIER

Available online at [www.sciencedirect.com](http://www.sciencedirect.com)

 ScienceDirect

Energy Procedia 4 (2011) 3628–3635

**Energy  
Procedia**

[www.elsevier.com/locate/procedia](http://www.elsevier.com/locate/procedia)

GHGT-10

## Geophysical monitoring of the Weyburn CO<sub>2</sub> flood: Results during 10 years of injection

D.J. White<sup>a,1</sup> for the Weyburn Geophysical Monitoring Team<sup>b</sup>

<sup>a</sup>Geological Survey of Canada, Ottawa, K1A 0E9, Canada

<sup>b</sup>M. Meadows, S. Cole (Fugro Seismic Imaging), A. Ramirez, Y. Hao, S. Carle (Lawrence Livermore National Lab), A. Duxbury, C. Samson (Carleton University), J.-M. Kendall, J.P. Verdon (Bristol University), B. Dietiker (Petroleum Technology Research Centre), J. Johnson (Schlumberger-Doll Research), I. Morozov (University of Saskatchewan),.

---

### Abstract

CO<sub>2</sub> monitoring activities within the IEA GHG Weyburn-Midale CO<sub>2</sub> Monitoring and Storage Project have been ongoing since 2000. Time-lapse seismic data provide the primary geophysical monitoring tool supplemented by passive microseismic monitoring. Here, we highlight results from seismic monitoring and the analysis methods applied to these data. Formal inversion methods (both prestack seismic inversion and model-based stochastic inversion) are being applied to optimize the geological model used to predict the storage behaviour of the reservoir. Seismic amplitude versus offset and azimuth analysis has been applied to identify areas of the caprock that may contain vertical fractures. Injection-related deformation of the reservoir zone has been modelled using coupled fluid flow-geomechanical modeling constrained by the observed low levels of microseismicity. Finally, we present results from a feasibility study on the use of electrical resistivity tomography for CO<sub>2</sub> monitoring at Weyburn using existing steel well casings as electrodes.

© 2011 Published by Elsevier Ltd.

*Keywords:* seismic; microseismic; geophysics; resistivity; inversion; monitoring

---

### 1. Introduction

The injection of CO<sub>2</sub> at EnCana's<sup>2</sup> Weyburn field began in 2000 as part of a miscible flood to enhance oil recovery. 2010 marks the 10th anniversary of the IEA GHG Weyburn-Midale CO<sub>2</sub> Monitoring and Storage Project whose focus has made Weyburn-Midale the most extensively studied CO<sub>2</sub> storage site in the world. More than 15 million tonnes of CO<sub>2</sub> have been stored at Weyburn since 2000, with current total field injection rates (new and recycled CO<sub>2</sub>) of 13,000 tonnes per day.

---

<sup>1</sup> Corresponding author. Tel: +1-613-992-0758; fax: +1-613-943-9285.  
E-mail address: [don.white@nrcan.gc.ca](mailto:don.white@nrcan.gc.ca).

<sup>2</sup> Originally PanCanadian and now Cenovus.

Subsequent to completion of Phase I of the project (see [1] for an overview) measurement, monitoring and verification activities have been continued in Phase II (2007–2011) of the project (see [2] for an overview of the original Phase II planned monitoring activities). As part of this, an extensive geophysical monitoring and analysis program has continued. In addition to acquiring new monitoring data, activities in Phase II of the project have focused on extracting as much information as possible from the new and existing monitoring data. This paper highlights some of the recent results and on-going work.

## 2. Time-lapse seismic monitoring

Geophysical monitoring at Weyburn has been spearheaded by time-lapse 3D seismic monitoring. The four time-lapse monitor surveys acquired from 2000–2007 have clearly identified the spread of CO<sub>2</sub> in the reservoir (e.g., [3]) where maximum associated decreases in acoustic impedance of 12% are observed in the immediate vicinity of horizontal CO<sub>2</sub> injection wells. Rock-fluid laboratory measurements show that a 12% impedance drop can be explained by a combination of increased pore pressure (~7 MPa) and CO<sub>2</sub> saturation.

The primary objective of the time-lapse seismic monitoring is to determine the subsurface distribution of CO<sub>2</sub>. This includes mapping the location of CO<sub>2</sub> within the primary injection zone (the reservoir), but also monitoring for CO<sub>2</sub> that is “out-of-zone”. The latter may occur either as a result of CO<sub>2</sub> leaking from the reservoir or alternatively as a result of out-of-zone injection. Time-lapse interval travel times provide a useful means of monitoring the overburden above the reservoir. Although they lack the resolving power of amplitude differences, they provide an integrated response of the entire interval. Seismic amplitudes though very sensitive to small changes in impedance, are also more prone to noise. Time-lapse interval travel times for the 2004 vs. the 2000 baseline survey are shown in Figure 2. The intervals are identified in relation to the reservoir in Figure 1. In comparing the two maps, the interval which

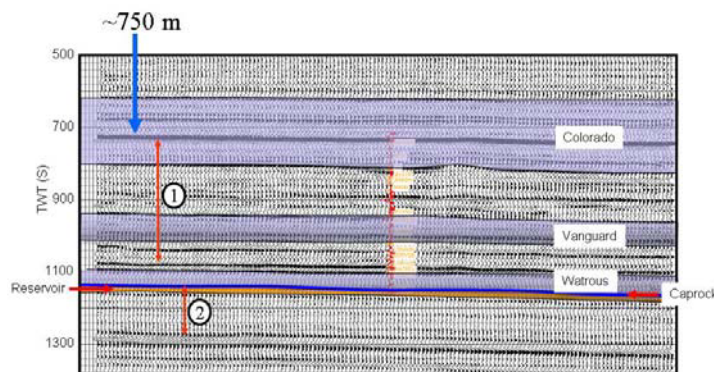


Figure 1. Weyburn seismic data. Purple intervals represent aquitards. Interval travel time differences have been determined for the intervals (1 and 2) as specified. The reservoir caprock is indicated in blue and the reservoir in orange.

includes the reservoir has pronounced negative travel time anomalies of up to ~2 ms that are clustered about the trajectories of the horizontal CO<sub>2</sub> injection wells. In contrast, there are few (if any) significant travel time anomalies in the interval above the regional seal (Watrous Formation [4]). Using the cumulative travel time delay and associated areal extent as a proxy for volume of CO<sub>2</sub> present, we can see that less than 1.5% of the injected CO<sub>2</sub> can be allocated to this large geological interval above the regional seal. The interval travel time changes observed in this upper interval may simply be noise, in which case there is no CO<sub>2</sub> above the regional seal. In any event, this exercise shows how the overburden interval can effectively be monitored seismically for large volumes of CO<sub>2</sub> that may have migrated upward.

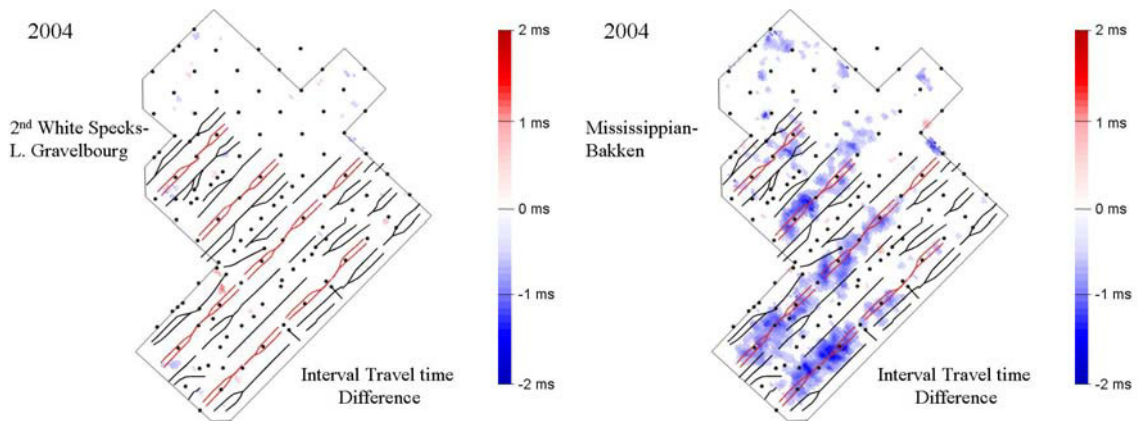


Figure 2 Interval travel time differences for intervals 1 and 2 as specified in Figure 1. a) Interval from top of regional seal (Watrous Formation) to 2<sup>nd</sup> White Speckled shale horizon, b) interval from the reservoir caprock (sub-Mesozoic unconformity) to Bakken including the reservoir interval. Horizontal CO<sub>2</sub> injection wells are indicated by red lines, horizontal production wells by black lines, and other wells (water injectors or production wells) by black dots.

### 3. Pressure vs. CO<sub>2</sub> saturation

One of the key challenges in utilizing the time-lapse seismic data to obtain semi-quantitative estimation of CO<sub>2</sub> saturations in the subsurface, is the discrimination of CO<sub>2</sub>-induced effects from pressure effects. In the Weyburn-Midale project, this issue is being tackled in several ways by: 1) Utilizing converted-wave (PS) data as a pressure discriminant. 2) Applying *amplitude-versus-offset* (AVO) analysis and inversion to prestack P-wave data. 3) Applying stochastic inversion methods to estimate the non-uniqueness and uncertainties in resultant CO<sub>2</sub> saturation estimates that are consistent with the data. Preliminary results from methods 2) and 3) are presented below.

*Prestack P-wave inversion:* Impedance inversion has been conducted on the different vintages of Weyburn Phase 1 time-lapse prestack seismic data to obtain P- and S-impedance volumes. The resultant time-lapse impedance changes have been used along with rock physics analysis on Weyburn samples, in a direct inversion procedure to obtain semi-quantitative estimates of pore pressure change and CO<sub>2</sub> saturation change within the reservoir zone. The applied inversion procedure is analogous to that described in [5] and [6], where impedances have been inverted instead of travel times and amplitudes, as in [7]. Preliminary inversion results for time slices of  $\Delta P_p$  and  $\Delta S_{CO_2}$  taken near the top of the reservoir (Marly unit) are shown in Figure 3. Maximum pore pressure increases of  $\sim 7$  MPa are observed, generally consistent with expected changes based on fluid flow simulations. Inversion results for CO<sub>2</sub> saturation changes are noisier than those for effective pressure changes as expected due to the ill-posed nature of the CO<sub>2</sub> inversion.

*Stochastic inversion:* In addition to the Phase 1 time-lapse seismic reflection data that has been used to map CO<sub>2</sub> migration [3], an extensive fluid sampling program has documented the concomitant geochemical evolution triggered by CO<sub>2</sub>-fluid-rock interactions [8]. The existing seismic and geochemical data sets—augmented by CO<sub>2</sub>/H<sub>2</sub>O injection and hydrocarbon/ H<sub>2</sub>O production data as well as additional Final-Phase monitoring results—are being used to improve both site characterization and dependent predictions of long-term storage performance at Weyburn. An inversion procedure is currently being developed that explicitly integrates reactive transport modeling, facies-based geostatistical methods, and a novel Monte Carlo Markov Chain (MCMC) stochastic inversion technique [9-11] to optimize agreement between observed and predicted storage performance. Such optimization will be accomplished through stepwise refinement of first the reservoir model—principally its permeability magnitude, anisotropy, and heterogeneity as constrained by the time-lapse seismic data—and then geochemical parameters—primarily key mineral volume fractions and kinetic data. It is anticipated that these refinements will facilitate significantly improved history matching and forward modeling of CO<sub>2</sub> storage.

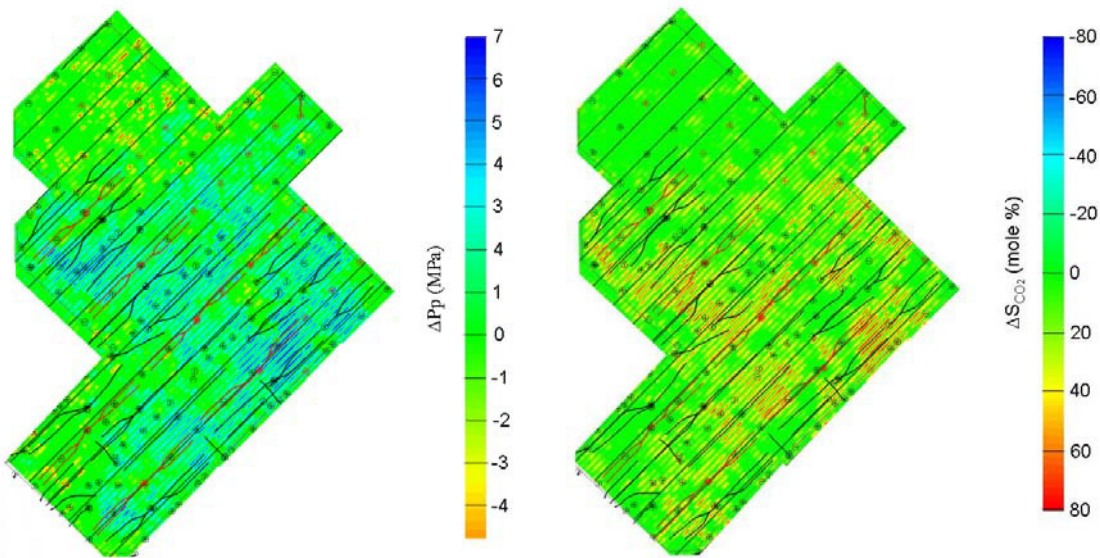


Figure 3 Time slices of  $\Delta P_p$  and  $\Delta S_{CO_2}$  taken near the top of the reservoir (Marly unit) A mild median filter has been applied to the difference volumes. Well patterns as in Figure 2.

To date, the seismic inversion component of the algorithm has been tested to evaluate its ability to recover reservoir model permeabilities that optimize agreement between measured and predicted seismic reflection data (see [12] for details of the methodology). A test reservoir model based on the Weyburn field model was constructed. Flow

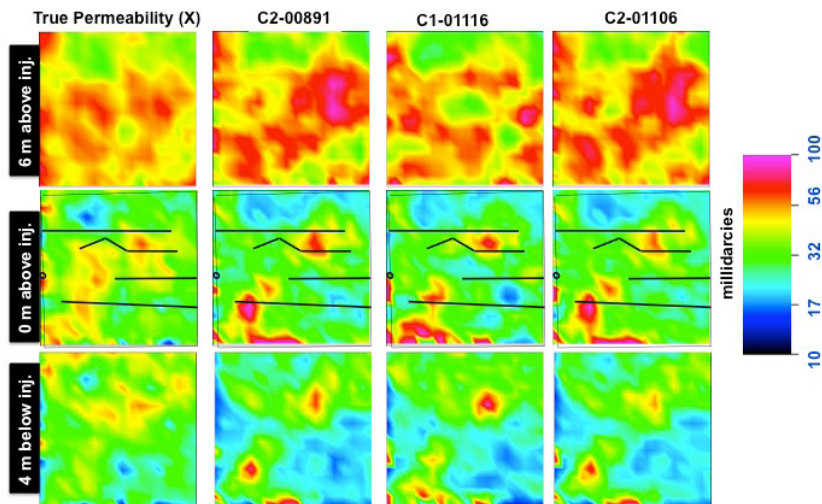


Figure 4. The left column of images shows horizontal slices through the true permeability model at 6m, 0m and -4 m above the horizontal injection well. The next three columns show recovered permeability distributions at each of the same levels that best fit the synthetic seismic data. The black lines indicate the location of horizontal wells.

simulations were conducted which matched the  $CO_2$  injection and fluid production rates used in the field. Synthetic seismic data determined for the resultant reservoir parameters (notably  $CO_2$  saturation, fluid densities, compressibilities and pore pressure) were used as the “observed data” for the stochastic inversion. The MCMC inversion software was then run to find permeability models that best fit the “observed” seismic data. Figure 4 shows a comparison of the permeability within the model used to generate the data in comparison to “optimal” permeability models. These are three model realizations within the Markov chain that was 1100 iterations long that have high corresponding likelihood values. As can be seen, the inversion models are characterized by some of the

same dominant trends as seen in the “true model”. The next step will be to apply the inversion tool to the actual observed time-lapse data from the Weyburn field.

#### 4. Caprock Integrity

The 3D seismic data have also been utilized to look for potential zones of fracturing within the reservoir caprock. Presently, there are few other practical means outside of extensive and costly core sampling to detect the presence of vertical fractures within the sealing unit(s) of potential geological storage sites. The presence of anisotropy within the caprock which may be fracture-related has been mapped using *amplitude-versus-offset-and-azimuth* (AVOA) techniques [13-14]. A map of seismic anisotropy determined for the caprock is shown in Figure 5, along with the associated orientations for zones where the anisotropy is high and the uncertainties are relatively low. Modelling results suggest that the trends in the northern half of the area are likely affected by anisotropy within the underlying reservoir as the caprock is relatively thin (< 20 m) in this area, and thus only those trends in the southern part of the area are considered reliable. These areas potentially represent zones of vertical fracturing, although we can't categorically state that they are fracture zones, or if they are, whether they are capable of transmitting fluids. However, they do represent target areas for focused surveillance during ongoing monitoring activities.

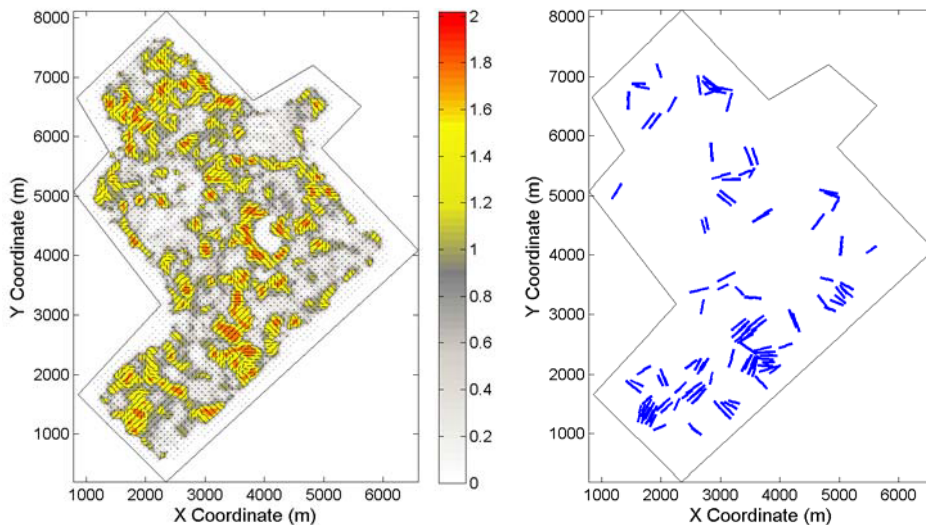


Figure 5. Right: normalized near-offset AVOA anisotropy magnitude from amplitude inversion of the cap rock horizon. Left: Residual anisotropy vectors for anisotropy with acceptable correlation, uncertainty and above average anisotropy. Only vectors in the southern (bottom) part of the area are considered as significant zones of anisotropy within the composite caprock zone.

#### 6. Microseismic monitoring & geomechanical modelling

Of the large-scale CCS pilot projects currently operational, thus far only the IEA GHG Weyburn-Midale CO<sub>2</sub> Monitoring and Storage Project has included passive seismic monitoring. Monitoring has been almost continuous from the deployment of the array in August, 2003 until the present. CO<sub>2</sub> injection in the adjacent injection well began in January of 2004. Detailed descriptions of the microseismic monitoring can be found elsewhere [1, 17-19]. Approximately 100 microseismic events have been located since the deployment of the array with 97% of the events occurring prior to early 2006 during the early stages of CO<sub>2</sub> injection. Microseismicity rates correlate with periods of elevated CO<sub>2</sub> injection rates, and also with changes in production activities in nearby production wells. Overall, the rate of seismicity is very low. Event magnitudes range from -3 to -1 in moment magnitude, with magnitude -2 events being detected at distances of up to 500 m. The lack of seismicity within the reservoir indicates that the reservoir is not undergoing significant geomechanical deformation or that it is doing so in a ductile manner.

The depth distribution of the microseisms is shown in Figure 7. Although the vertical locations are subject to relatively large uncertainties (at least  $\pm 70$  m in some cases), it appears that a large number of events occur outside of the reservoir. This observation could raise concern as it might be indicative of CO<sub>2</sub> leakage or direct hydraulic communication of the reservoir and overburden. However, coupled fluid flow-geomechanical simulations for a Weyburn-based model conclude that seismicity immediately above the reservoir is likely due to stress-arching effects rather than CO<sub>2</sub> escaping from the reservoir [19]. Furthermore, the location of microseismicity is controlled by pressure-induced stress changes in the reservoir which in general are not directly related to the distribution of CO<sub>2</sub>. This indicates that passive monitoring will be useful primarily for monitoring deformation that could compromise the integrity of the reservoir seal. In the case of the Weyburn, the microseismic event uncertainties are too large to determine whether the events occur within the reservoir caprock.

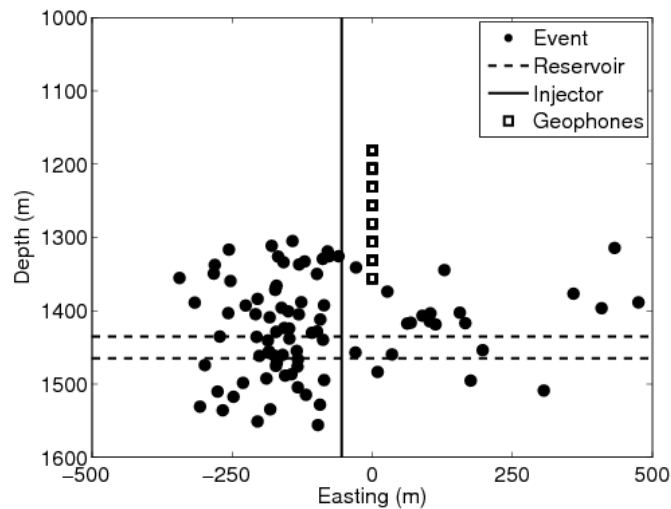


Figure 6. Complete set of microseismic event locations in cross-section. The seismic array is marked by the bold squares and the vertical injection well is indicated by the solid vertical line.

## 5. Long Electrode Electrical Resistance Tomography (LEERT) Modelling

Electrical sounding methods potentially provide an alternate means of monitoring the subsurface distribution of injected CO<sub>2</sub> [18]. Where metal-cased boreholes are available, they can be used as long electrodes for electrical resistivity imaging (*e.g.*, [11]). The objective is to produce time dependent maps of changes in formation resistivity caused by CO<sub>2</sub> injection and migration. A numerical modeling study has been conducted to evaluate whether LEERT could be used successfully to monitor CO<sub>2</sub> distribution in the Weyburn-Midale reservoir, Phase 1B area. We consider two injection volume scenarios for this study (refer to Figure 7). One case assumes injection over a 1.4 year period and another case assumes injection over a 5.7 year period. We assume that the CO<sub>2</sub> causes a fourfold increase in resistivity [19]. We also assume that the reservoir layer is more resistive than layers above and below based on electrical logs from the Weyburn site.

The modelling results suggest that none of the deployment scenarios considered are likely to produce enough data with adequate signal-to-noise ratio and sensitivity to allow successful inversion of ERT data. This is mostly due to the challenging conditions present at the Phase 1B area which include long casings, large depth to reservoir, the reservoir layer being more resistive than the overburden, the presence of other casings that distort the field, and the large inter-electrode distance. Of these factors, the large inter-electrode distances are considered the greatest limitation. The modeling also illustrates that: a) Low current densities in the reservoir layer tend to produce measurements with low signal-to-noise ratio. b) Sensitivity is greatly reduced in the inter-electrode regions. c)

Sensitivity is inversely proportional to casing length. d) The presence of other metallic casings distort the current field which directly affects the capacity to resolve the shape of the CO<sub>2</sub> plume.

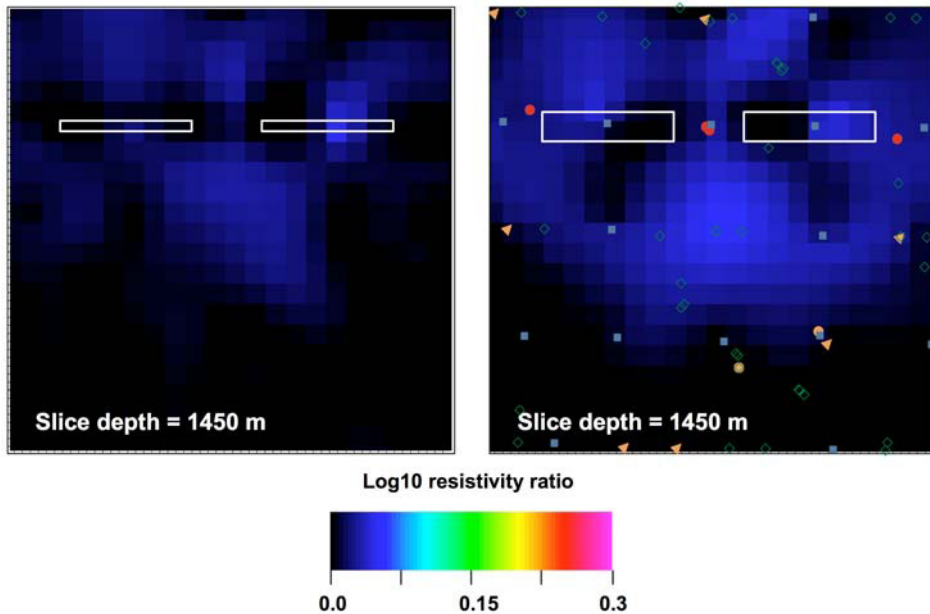


Figure 7. Resistivity changes recovered using synthetic data. The data were calculated for acquisition using 22 well casings; 8 abandoned wells (orange triangles) and 22 active vertical wells (blue squares). All wells end at the top of the reservoir (1420 m). The left and right images show resistivity changes due to 1.4 and 5.7 years of injection, respectively., with the white outlines showing the extent and location of the CO<sub>2</sub> from the simulation. The true resistivity ratio is  $\log_{10}(4) = 0.6$ .

## 7. Acknowledgements

## References

1. White, D.J., Hirsche, K., Davis, T., Hutcheon, I., Adair, R., Burrowes, G., Graham, S., Bencini, R., Majer, E., and Maxwell, S.C., 2004. Theme 2: Prediction, Monitoring and Verification of CO<sub>2</sub> movements, Chapter 3 (p. 73-148), in IEA GHG Weyburn CO<sub>2</sub> Monitoring and Storage Project Summary Report 2000-2004, From the proceedings of the 7<sup>th</sup> International Conference on Greenhouse Gas Control Technologies, edited by M. Wilson, M. Monea, Petroleum Technology Research Centre, Regina.
2. White, D.J., and Johnson, J.W., 2008. Integrated Geophysical and Geochemical Monitoring Programs of the IEA GHG Weyburn-Midale CO<sub>2</sub> Monitoring and Storage Project, Energy Procedia, Volume 1, Issue 1, February 2009, Pages 2349-2356, Greenhouse Gas Control Technologies 9, Proceedings of the 9<sup>th</sup> International Conference on Greenhouse Gas Control Technologies (GHGT-9), 16–20 November 2008, Washington DC, USA.
3. White, D., 2009. Monitoring CO<sub>2</sub> storage during EOR at the Weyburn-Midale field. *The Leading Edge* 28, 838–842.
4. Whittaker, S., Rostron, B., Khan, D., Hajnal, Z., Qing, H., Penner, L., Maathuis, H., and Goussev, S., 2004. Theme 1: Geological Characterization, Chapter 2 (p. 15-72), in IEA GHG Weyburn CO<sub>2</sub> Monitoring and Storage Project Summary Report 2000-2004, From the proceedings of the 7<sup>th</sup> International Conference on Greenhouse Gas Control Technologies, edited by M. Wilson, M. Monea, Petroleum Technology Research Centre, Regina.
5. Cole, S., Lumley, D., Meadows, M., and Tura, A., 2002. Pressure and saturation inversion of 4D data by rock physics forward modeling: 72<sup>nd</sup> Annual International Meeting, Society of Exploration Geophysicists, Expanded Abstracts, 2475-2478.

6. Lumley, D., Adams, D., Meadows, M., Cole, S., and Ergas, R., 2003. 4D seismic pressure-saturation inversion at Gullfaks field, Norway, *First Break*, 21, 49-56.
7. Meadows, M., 2008, Time-lapse seismic modeling and inversion of CO<sub>2</sub> saturation for storage and enhanced oil recovery: The Leading Edge, April, 506-515.
8. Shevalier, M., Durocher, K., Perez, R., Hutcheon, I., Mayer, B., Perkins, E., and Gunter, W., 2005. Geochemical monitoring of gas-water-rock interaction at the IEA Weyburn CO<sub>2</sub> Monitoring and Storage Project, Saskatchewan, Canada. Proceeding of the 7th International Conference on Greenhouse Gas Control Technologies, Vol. II – Part 2, Poster Papers, edited by Wilson, M., Morris, T., Gale, J., and Thambimuthu, K., Elsevier, 2135-2139.
9. Aines, R.D., J.J. Nitao, R.L. Newmark, S. Carle, A.L. Ramirez, D.B. Harris, J.W. Johnson, V.M. Johnson, D. Ermak, G. Sugiyama, W.G. Hanley, S. Sengupta, W. Daily, R. Glaser, K. Dyer, G Fogg, Y. Zhang, Z. Yu, R. Levine, 2002, The Stochastic Engine Initiative: Improving Prediction of Behavior in Geologic Environments We Cannot Directly Observe, UCRL-ID-148221, Lawrence Livermore National Laboratory, Livermore, CA.
10. Ramirez, A. L., J.J. Nitao, W.G. Hanley, R.D. Aines, R.E. Glaser, S.K. Sengupta, K.M. Dyer, T.L. Hickling, W.D. Daily, 2005, Stochastic Inversion of Electrical Resistivity Changes Using a Markov Chain, Monte Carlo Approach, *Journal of Geophysical Research*, Vol. 110, B02101, doi: 10.1029/2004JB003449.
11. Daily, W., Ramirez, A., Newmark, R., and Masica, K., 2004. Low-cost tomographs of electrical resistivity, The Leading Edge, Society of Exploration Geophysicists, 472-480.
12. Ramirez, A., Y. Hao, D. White, S. Carle, K. Dyer, X. Yang, W. Foxall, and J. Johnson, 2010. Optimizing the Weyburn-Midale reservoir model using the seismic response to CO<sub>2</sub> Injection and Stochastic Inversion, Proceedings of the 9<sup>th</sup> Annual Conference on Carbon Capture & Sequestration, Pittsburgh.
13. Duxbury, A., 2010. Fracture detection using seismic anisotropy at the Weyburn CO<sub>2</sub> storage site, Saskatchewan, M.Sc. thesis, Carleton University, 115 p.
14. Duxbury, A., White, D., Samson, C., Hall, S., Wookey, J., and Kendall, J-M., 2010. Fracture detection using AVOA for cap-rock assessment in the Weyburn-Midale CO<sub>2</sub> monitoring and storage project, 2010 Society of Exploration Geophysicists Annual Meeting Expanded Abstracts, Denver.
15. Maxwell, S.C., White, D.J., and Fabriol, H., 2005. Passive seismic imaging of CO<sub>2</sub> sequestration at Weyburn, 67th EAGE Conference and Exhibition, Madrid, Spain, expanded abstract, 4p.
16. Deflandre, J.-P., Andonof, L.J., Fabriol, H., and White, D., 2006. Induced microseismicity and CO<sub>2</sub> injection at the Weyburn oil field: improvement in source locations, *In* Proceedings of the 8th International Conference on Greenhouse Gas Control Technologies, Trondheim, Norway, 3p.
17. Verdon, J.P., Kendall, J-M., White, D.J., and Angus, D.A., 2010. Linking microseismic event observations with geomechanical models to minimise the risks of storing CO<sub>2</sub> in geological formations, submitted to *Earth and Planetary Science Letters*.
18. Ramirez, A., Newmark, R., and Daily, W., 2003. Monitoring carbon dioxide floods using electrical resistance tomography (ERT): Sensitivity studies, *Journal of Environmental and Engineering Geophysics*, v. 8, no. 3, 187-208..
19. Albright, J. C., 1986, Use of well logs to characterize fluid flow in the Maljamar CO<sub>2</sub> Pilot, *J. Pet. Tech.*, vol. 38, no. 9, p. 883, 890.